Available online at www.sciencedirect.com
ScienceDirect
Journal of Power Sources 159 (2006) 233–236
JOURNAL OF POWER SOURCES
www.elsevier.com/locate/jpowsour

Short communication

Crystal structures, electrical conductivities and electrochemical properties of $LiCo_{1-x}Mg_xO_2$ ($0 \leq x \leq 0.11$)

Ho-Jin Kim, Yeon Uk Jeong, Joon-Hyung Lee, Jeong-Joo Kim *

Department of Inorganic Materials Engineering, Kyungpook National University, Daegu 702-701, Korea

Available online 26 May 2006

Abstract

$LiCoO_2$ is commercially available cathode electrode materials of lithium-ion batteries. In an attempt to improve the performance of lithium batteries with enhanced safety, $LiCo_{1-x}Mg_xO_2$ was synthesized by the solid-state reaction method. The crystal structure was analyzed by X-ray diffraction and Rietveld refinement. $LiCo_{1-x}Mg_xO_2$ give a single phase of a layered structure with the space group *R*-3*m* of hexagonal systems for $x \leq 0.11$. A second phase of MgO was observed in $LiCo_{1-x}Mg_xO_2$ for $x \geq 0.13$. The calculated cation–anion distances and angles from the Rietveld refinement were changed with Mg content in samples. With the increase in Mg content in $LiCo_{1-x}Mg_xO_2$, distances between CoO_2 slabs were increased. The electrical conductivities of sintered samples were measured at room temperature by the Van der Pauw method. The electrical conductivities of $LiCo_{1-x}Mg_xO_2$ increased with Mg content. On the basis of the Hall effect analysis, the increase in electrical conductivities with Mg content is believed due to the increased carrier concentrations, while the carrier mobility was almost invariant with the Mg content. The electrochemical performance of $LiCo_{1-x}Mg_xO_2$ was evaluated by coin cell test.

Keywords: Li-ion batteries; Mg doping; Rietveld refinement; Electrical conductivity

1. Introduction

Rechargeable lithium batteries are very attractive power sources as they offer higher energy and power density than other rechargeable battery systems [1,2]. $LiCoO_2$ for cathode material is commercially available in the market as it has high energy density and good cycle life [3]. Environmental and safety concerns of lithium batteries need alternate materials with enhanced performances. Research and development efforts have been directed towards improvements in the materials and processes. In the case of $LiNiO_2$, it is difficult to synthesize an highly ordered form and exhibits thermal instability [4,5]. For $LiMn_2O_4$, in spite of low cost and environmental friendliness, it suffers from limited theoretical capacity, low density and poor cycling performances [6]. Improved performances of $LiCoO_2$, $LiNiO_2$ and $LiMn_2O_4$ have been achieved by doping with divalent and trivalent metal ions. Doping of Zr, Al, Mg in $LiCoO_2$ were reported to enhance structural stability and cycling performance [7–9]. Mg-doped $LiCoO_2$ exhibits an enhanced electrical conductivity at room temperature [9]. Recently, in attempt to increase capacity, a method of charging at higher voltage (>4.3 V) has been pursued. In this regard, thorough studies on structural characteristics of doped-$LiCoO_2$ as well as structural stabilities of delithiated cathodes are thought to be essential.

This paper describes the systematical investigation for exact solubility of Mg in $LiCoO_2$, the detail structural characteristics, electrical conductivities and electrochemical properties.

2. Experimental

$LiCo_{1-x}Mg_xO_2$ ($x = 0$–0.15) samples were synthesized by solid-state reactions. Li_2CO_3, Co_3O_4 and MgO as starting materials were milled with zirconia ball in acetone for 24 h. The ratio of Li:(Co + Mg) was adjusted to 1.05:1, considering lithium loss at high synthesis temperature. After acetone was removed and dried, powder mixture was heated at 800 °C for 12 h in air. X-ray powder diffraction and Rietveld analysis were used to analyze the crystal structures of products. Especially, structure analyses were focused on the distances and angles between ions. Van der Pauw method and Hall effect measurement system was used to evaluate electrical conductivities of samples at room temperature.

* Corresponding author. Tel.: +82 53 950 5635; fax: +82 53 950 5645.
E-mail address: jjkim@knu.ac.kr (J.-J. Kim).

0378-7753/$ – see front matter © 2006 Elsevier B.V. All rights reserved.
doi:10.1016/j.jpowsour.2006.04.030

The electrochemical performances were evaluated by using a coin-type cell (size 2016). Composite cathode films were prepared by mixing of 95 wt% active material, 2 wt% acetylene black as a conductive additive and 3 wt% polyvinylidene fluoride (PVDF) as a binder, and *N*-methyl pyrrolidone (NMP) as a solvent. Lithium metal was used as anode. For electrolytes, 1.15 M $LiPF_6$ was dissolved in the solution of ethylene carbonate (EC), dimethyl carbonate (DMC) and diethyl carbonate (DEC) with ratio of 3:6:1. The galvanostatic charge/discharge test was performed between 4.3 V and 3.0 V with different current densities (0.1 C, 0.2 C, 0.5 C, 1 C, 2 C), and 1 C rate was 140 mAh g^{-1}.

3. Results and discussions

3.1. Synthesis and structure analysis of $LiCo_{1-x}Mg_xO_2$ ($0 \le x \le 0.15$)

Synthesized $LiCo_{1-x}Mg_xO_2$ phases were characterized by X-ray powder diffraction. Fig. 1 shows XRD patterns for $LiCo_{1-x}Mg_xO_2$ ($0 \le x \le 0.15$). While $LiCo_{1-x}Mg_xO_2$ ($x \le 0.11$) samples show layered structure of single phase $LiCoO_2$, impurity phase of MgO was found in $LiCo_{1-x}Mg_xO_2$ ($x \ge 0.13$) samples. The results of Rietveld refinement are shown in Fig. 2. Lattice constants and specific positions of oxygen of each sample are summarized in Table 1. Lattice constants of *a* and *c*-axis were increased with increase in Mg contents in $LiCo_{1-x}Mg_xO_2$ ($x \le 0.11$) samples. According to Delmas and co-workers [10], lattices constants were increased due to the replacement of larger Mg ions instead of Co ions ($r_{Mg^{2+}} = 0.72$Å , $r_{Co^{3+}} = 0.545$Å , $r_{Co^{4+}} = 0.53$Å). Bond lengths and angles between anion and cations are shown in Table 2. Crystal structure of $LiCo_{1-x}Mg_xO_2$ is drawn in Fig. 3. Bond lengths of Li–O and Co–O were increased with increasing Mg content in the samples. With the increase in Mg content in $LiCo_{1-x}Mg_xO_2$, O_1–Li–O_2 and O_1–Co–O_4 angles were decreased, O_1–Li–O_4 and O_1–Co–O_2 angles were increased. Increase in Mg amount of samples resulted in decrease in the thickness of CoO_2 slab and increase in the distance of inter-slab (Fig. 4). Larger inter-slab distance might help to facilitate the intercalation and de-intercalation of lithium ions in the lattice.

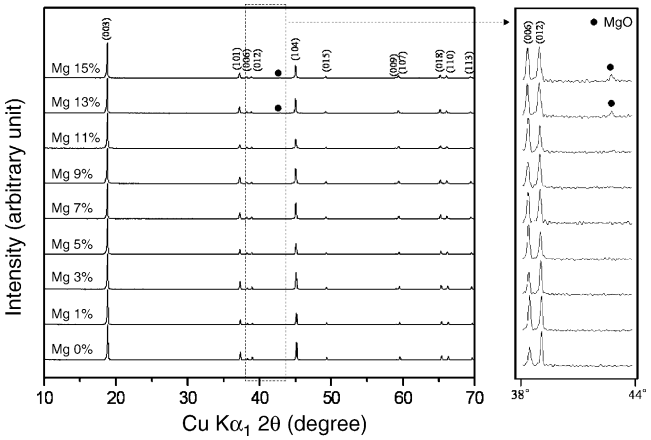

Fig. 1. X-ray powder diffraction patterns of $LiCo_{1-x}Mg_xO_2$ phases.

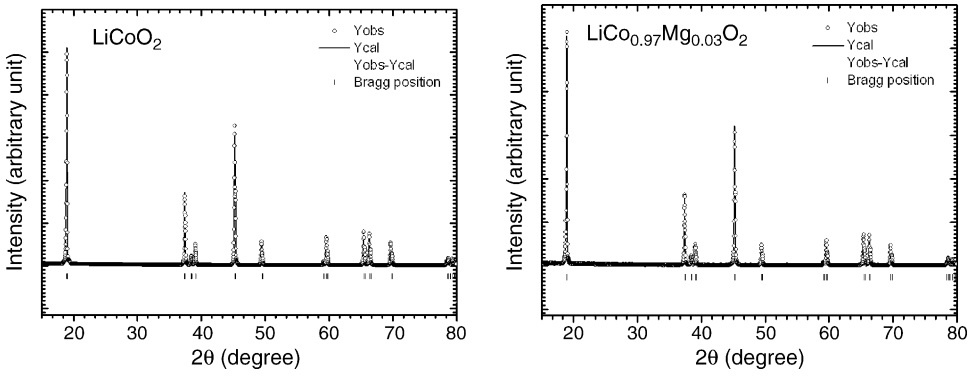

Fig. 2. XRD patterns of $LiCoO_2$ and $LiCo_{0.97}Mg_{0.03}O_2$ phases by Rietveld refinement.

Table 1
Hexagonal cell parameters and position of oxygen *Z* from Reitveld refinement for the different $LiCo_{1-x}Mg_xO_2$ samples

Compound	$a_{hex.}$ (Å)	$c_{hex.}$ (Å)	*c*/*a*	Z_{oxygen}	R_p	Chi^2
$LiCoO_2$	2.81417	14.04346	4.990	0.23970	8.78	1.86
$LiCo_{0.99}Mg_{0.01}O_2$	2.81483	14.04570	4.990	0.23966	8.38	1.86
$LiCo_{0.97}Mg_{0.03}O_2$	2.81638	14.05293	4.990	0.23953	8.26	1.75
$LiCo_{0.95}Mg_{0.05}O_2$	2.81819	14.06194	4.990	0.23940	8.60	1.86
$LiCo_{0.93}Mg_{0.07}O_2$	2.81975	14.06908	4.989	0.23937	8.76	1.96
$LiCo_{0.91}Mg_{0.09}O_2$	2.82039	14.07258	4.990	0.23934	7.99	1.95
$LiCo_{0.89}Mg_{0.11}O_2$	2.82109	14.07715	4.990	0.23930	8.70	2.10
$LiCo_{0.087}Mg_{0.13}O_2$	2.82178	14.07792	4.989	0.23574	12.00	3.37
$LiCo_{0.85}Mg_{0.15}O_2$	2.82188	14.07798	4.989	0.23555	11.90	3.22

Table 2
The calculated cation–anion distances and angles from Rietveld refinement for $LiCo_{1-x}Mg_xO_2$ samples

Compound	Distance (Å)		Angle (°)	
	Li–O	Co–O	O_1–Li–O_2/O_1–Li–O_4	O_1–Co–O_2/O_1–Co–O_4
$LiCoO_2$	2.0902	1.9214	84.63/95.37	94.16/85.84
$LiCo_{0.99}Mg_{0.01}O_2$	2.0910	1.9215	84.61/95.39	94.18/85.82
$LiCo_{0.97}Mg_{0.03}Q_2$	2.0932	1.9216	84.56/95.44	94.25/85.75
$LiCo_{0.95}Mg_{0.05}O_2$	2.0957	1.9218	84.50/95.50	94.31/85.69
$LiCo_{0.93}Mg_{0.07}O_2$	2.0971	1.9227	84.49/95.51	94.33/85.67
$LiCo_{0.91}Mg_{0.09}O_2$	2.0979	1.9229	84.48/95.53	94.34/85.66
$LiCo_{0.89}Mg_{0.11}O_2$	2.0988	1.9231	84.45/95.55	94.36/85.64

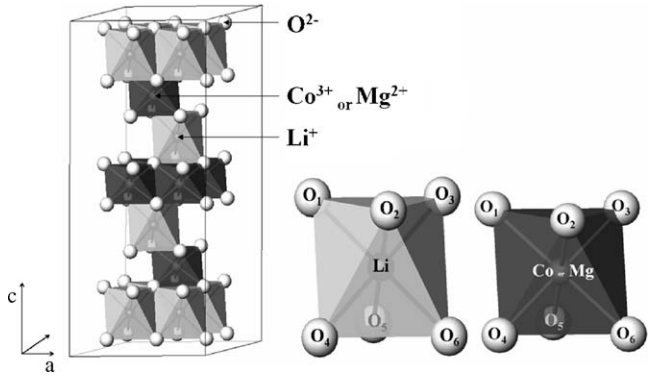

Fig. 3. Structure of $LiCo_{1-x}Mg_xO_2$.

3.2. Electrical conductivities of $LiCo_{1-x}Mg_xO_2$ ($0 \le x \le 0.11$)

Electrical conductivity, carrier concentration and carrier mobility of sintered $LiCo_{1-x}Mg_xO_2$ samples were evaluated by of Van der Pauw method and Hall Effect Measurement System. Electrical properties are shown in Fig. 5(a). According to Tukamoto and West, increase in electrical conductivities of $LiCo_{1-x}Mg_xO_2$ is due to the generation of holes [9]. While carrier concentrations were increased with increase in Mg content, carrier mobilities remain constant. Hence enhancement of electrical conductivities in $LiCo_{1-x}Mg_xO_2$ were mainly due to the increase in the concentration of holes. Electrical conductivities of $LiCoO_2$ and $LiCo_{0.97}Mg_{0.03}O_2$ were 2.11×10^{-4} S cm^{-1} and 2.41×10^{-1} S cm^{-1}, respectively. However, large increases in electrical conductivities were not found in $LiCo_{1-x}Mg_xO_2$

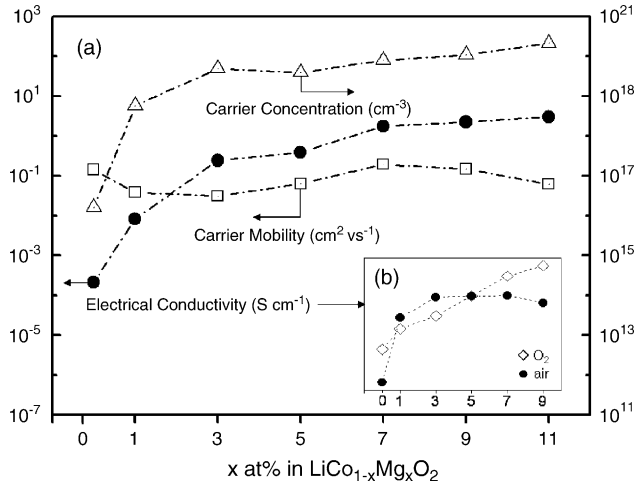

Fig. 5. Electrical properties in $LiCo_{1-x}Mg_xO_2$ as a function Mg content: (a) electrical conductivities, carrier concentrations and carrier mobilities and (b) electrical conductivities in oxygen and air atmosphere.

($x = 0.03$–0.11). This might be due to the formation of oxygen vacancies in the lattice and reduction of hole concentration. Therefore, heating in O_2 atmosphere might help to prevent oxygen deficiency in the lattice. Effect of the heating at different atmospheres is shown in Fig. 5(b).

3.3. Electrochemical performances

Charge and discharge profiles of $LiCo_{1-x}Mg_xO_2$ ($0 \le x \le 0.07$) are shown in Fig. 6. $LiCo_{0.97}Mg_{x.03}O_2$ shows discharge capacities of 169 mAh g^{-1} and 161 mAh g^{-1} at 0.1 C and 1 C,

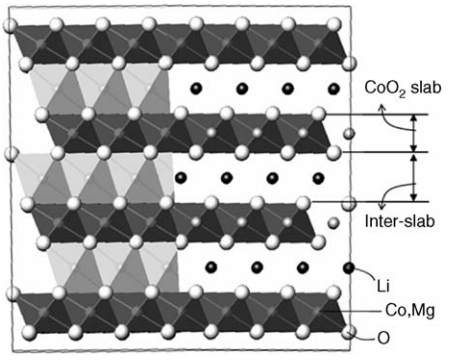

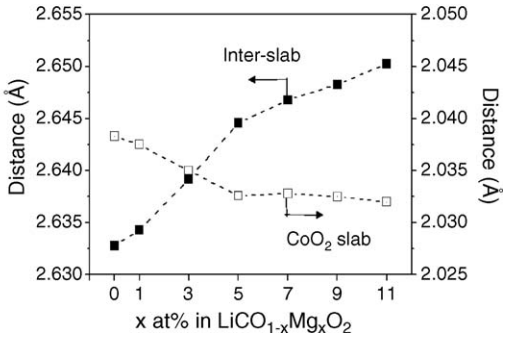

Fig. 4. The calculated CoO_2 slab and inter-slab distances from Rietveld refinement as a function of Mg content.

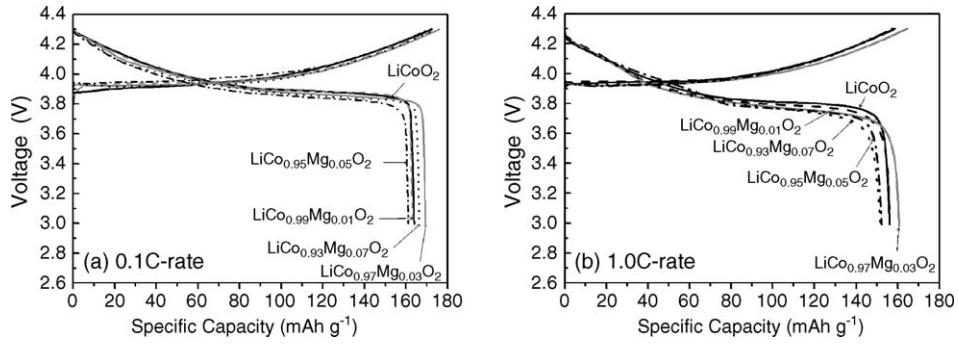

Fig. 6. (a and b) Charge–discharge profiles of $LiCo_{1-x}Mg_xO_2$ ($x = 0$, 0.01, 0.03, 0.05, 0.07).

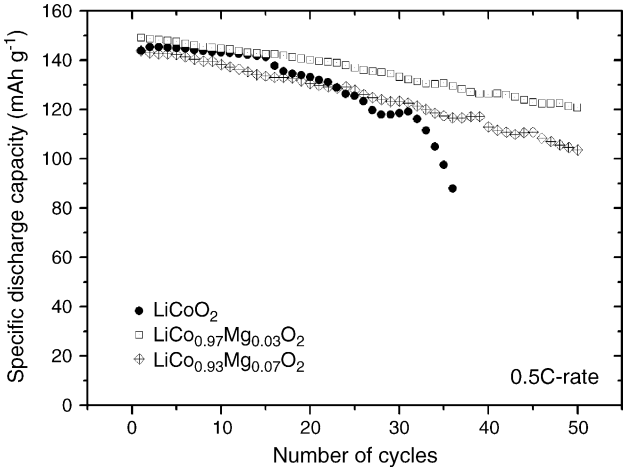

Fig. 7. Cycling performances of $LiCoO_2$, $LiCo_{0.97}Mg_{0.03}O_2$ and $LiCo_{0.93}Mg_{0.07}O_2$ at 0.5 C-rate (voltage range: 3.0–4.3 V).

respectively. Results of cyclability test of $LiCo_{1-x}Mg_xO_2$ ($x = 0$, 0.03, 0.07) are shown in Fig. 7. $LiCo_{0.97}Mg_{x.03}O_2$ sample exhibited improved cycle life compared to $LiCoO_2$. Enhancement in cycle performance might be due to the improved electrical conductivity as well as increase in inter-slab distance.

4. Conclusions

$LiCo_{1-x}Mg_xO_2$ were synthesized by solid-state reaction. The solubility limit of MgO in $LiCoO_2$ was 11 at%. With increase in Mg content in $LiCo_{1-x}Mg_xO_2$, lattice constants (a, c) and bond lengths (Co–O, Li–O) were increased, bond angles (O–Co–O, O–Li–O) were changed, and distances between CoO_2 slabs were increased. Improved electrical conductivities of $LiCo_{1-x}Mg_xO_2$ were due to the concentration of hole. Heating at various oxygen partial pressures could control the amount of oxygen vacancy in $LiCo_{1-x}Mg_xO_{2-\delta}$. $LiCo_{1-x}Mg_xO_2$ ($x = 0.03$, 0.07) samples exhibit better cyclabilities than $LiCoO_2$, this might be due to the improved electrical conductivity as well as increase in inter-slab distance.

Acknowledgements

This work was supported by the National Research Laboratory grant from the Ministry of Science and Technology (MOST) and Korea Science and Engineering Foundation (KOSEF).

References

[1] M. Armand, Solid State Ionics 69 (1994) 309–319.
[2] H.V. Venkatasetty, J. Power Sources 97–98 (2001) 671–673.
[3] M. Yoshio, H. Tanaka, K. Tomonaga, H. Noguchi, J. Power Sources 40 (1992) 347–353.
[4] A. Rougier, P. Gravereau, C. Delmas, J. Electrochem. Soc. 143 (1996) 1168–1175.
[5] H. Arai, S. Okada, Y. Sakurai, J. Yamaki, Solid State Ionics 109 (1998) 295–302.
[6] T. Inoue, M. Sano, J. Electrochem. Soc. 145 (1998) 3704–3707.
[7] C. Julien, G.A. Nazir, A. Rougier, Solid State Ionics 135 (2000) 121–130.
[8] T.-S. Kim, T.-K. Ko, B.-K. Na, W.I. Cho, B.W. Chao, J. Power Sources 138 (2004) 232–239.
[9] H. Tukamoto, A.R. West, J. Electrochem. Soc. 144 (1997) 3164–3168.
[10] S. Levasseur, M. Menetrier, C. Delmas, Chem. Mater. 14 (2002) 3584–3590.